



ELSEVIER

International Journal of Mass Spectrometry 185/186/187 (1999) 327–341



Gas phase and condensed phase S_Ni reactions. The competitive five and six centre cyclisations of the 4,5-epoxy-pentoxide anion: a joint experimental and theoretical study

John M. Hevko, Suresh Dua, Mark S. Taylor, John H. Bowie*

Department of Chemistry, The University of Adelaide, 5005 South Australia

Received 5 June 1998; accepted 20 July 1998

Abstract

Ab initio calculations [at the MP2 Fc/6-31+G(d) level of theory] indicate that the barriers to the transition states for the competitive five and six centre S_Ni cyclisation processes of the 4,5-epoxy-pentoxide anion are both 48 kJ mol^{-1} . Experimental studies show that (1) in solution, the 4,5-epoxy-pentoxide anion cyclises (and at the same time opens the ethylene oxide ring) to give tetrahydrofurfuryl alcohol [tetrahydro-2-furanmethanol (the product of the five-centre cyclisation)] as the predominant product on workup, and (2) collision activation of the 4,5-epoxy-pentoxide anion in the gas phase gives the tetrahydro-2-furanmethoxide anion as the exclusive product. Since the computed barriers for the cyclisations proceeding through five- and six-membered transition states are comparable, frequency factors (Arrhenius A factors) must be controlling the courses of the kinetically controlled reactions. A comparison of the calculated harmonic vibrational partition functions for the two transition states confirms a higher value of A (and hence a higher rate) for the reaction proceeding via the five-membered transition state. (Int J Mass Spectrom 185/186/187 (1999) 327–341) © 1999 Elsevier Science B.V.

Keywords: S_Ni reactions; 4,5-epoxy-pentoxide anion; Condensed and gas phase comparison

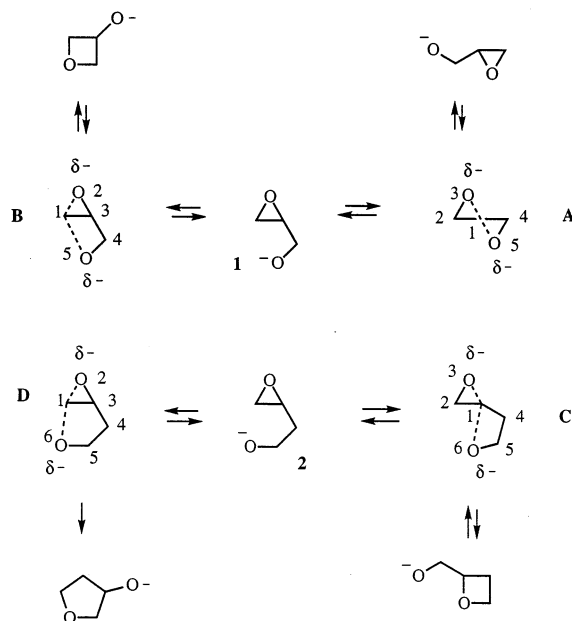
1. Introduction

Previous studies have shown that the relative rates of two competing gas phase S_Ni reactions of ethylene oxides are dependent on a number of factors, including (1) the angle of approach of each nucleophile to the receptor atom (the closer to 180° , the more favourable the reaction), and (2) the relative ring strain energies involved in forming the two transition states [1–3].

Our previous work with epoxides is summarised in Scheme 1. (A reviewer has asked whether these gas phase results agree with Baldwin's rules. The particular rule involves base-catalysed solution-phase reactions of ethylene oxides substituted with a side chain that contain a stabilised carbanion: in cases where competitive S_Ni reactions may occur via the carbanion, that producing the smaller ring is predominant [4–6]. We have not studied the analogous carbanion cyclisations in the gas phase so we cannot comment on those systems, however, with the exception of our 4/5 system [3], the results shown in Scheme 1 show a similar trend to those obtained for Baldwin's carbanion examples [5].) The energised 2,3-epoxypropoxide

* Corresponding author.

Dedicated to Michael T. Bowers on the occasion of his 60th birthday.



Scheme 1.

$$\text{A, } C_1O_3 = C_1O_5 = 1.89 \text{ \AA}; \quad O_3C_1O_5 = 160.1^\circ; \quad O_5C_1C_2O_3 = -159.7^\circ$$

$$\text{B, } C_1O_2 = 1.91; \quad C_1O_6 = 2.08 \text{ \AA}; \quad O_2C_1O_6 = 116.5^\circ; \quad O_6C_1C_3O_2 = -153.0^\circ$$

$$\text{C, } C_1O_3 = 1.85; \quad C_1O_6 = 2.00 \text{ \AA}; \quad O_3C_1O_6 = 163.4^\circ; \quad O_6C_1C_2O_3 = -163.1^\circ$$

$$\text{D, } C_1O_2 = 1.84; \quad C_1O_6 = 2.09 \text{ \AA}; \quad O_2C_1O_6 = 140.4^\circ; \quad O_6C_1C_3O_2 = -163.1^\circ$$

anion (**1**) undergoes the two competitive reactions shown, with the Payne rearrangement (through transition state **A**) predominating: here, the relative ring strain energies are not a major factor (the respective strain energies for ethylene oxide and oxetan are 112.5 and 107.5 kJ mol⁻¹ [7]). In contrast, the 3,4-epoxybutoxide anion (**2**) proceeds to transition states **C** and **D** to comparable extents: the O–C–O angles in the transition states favour reaction through **C** (see Scheme 1), while **D** is favoured because the ring strain is less (the respective ring strains for oxetan and tetrahydrofuran are 107.5 and 25 kJ mol⁻¹ [7]). There is no evidence of frequency factors being major influences in determining relative rates of the studied reactions [3].

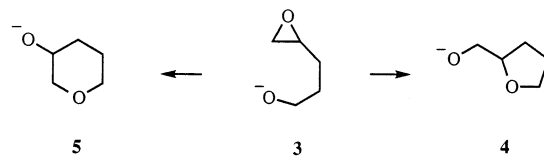
In this article we extend the above studies to probe the scenario outlined in Scheme 2. Does the 4,5-epoxypentoxide anion (**3**) form **4** and **5** in both the gas and condensed phases? Is the angle of approach of O⁻

to each of the electrophilic carbon atoms the major factor influencing the reactions (the difference in strain energies are modest: the relative strain energies of tetrahydrofuran and tetrahydropyran being 25 and 6 kJ mol⁻¹ [7])?

2. Experimental

2.1. Mass spectrometric methods

Collisional activation (CA) mass spectra (MS/MS) were determined with a VG ZAB 2HF mass spec-



Scheme 2.

trometer [8]. Full operating details have been reported [9]. Specific details were as follows: the chemical ionisation slit was used in the chemical ionisation source, the ionising energy was 70 eV, the ion source temperature was 100°C, and the accelerating voltage was 7 kV. The liquid samples were introduced through the septum inlet with no heating [measured pressure of sample 1×10^{-6} Torr (1 Torr = 133.322 Pa)]. Alkoxide anions were formed by S_N2 displacement from the appropriate methyl ether using HO^- (from H_2O : measured pressure 1×10^{-5} Torr). The estimated source pressure was 10^{-1} Torr. Argon was used in the second collision cell (measured pressure, outside the cell, 2×10^{-7} Torr), giving a 10% reduction in the main beam, equivalent to single collision conditions. (CA) MS/MS measurements involved using the magnet to choose the ion under study [normally the $(M-H)^-$ species], collision activating it (see above), and scanning the electric sector to analyse the resultant product anions. Charge reversal (CR) (positive ion) MS/MS data for negative ions were obtained as for CA MS/MS data, except that the electric sector potential was reversed to allow the transmission of positively charged product ions (for full details see [10]). The recorded peak widths at half height are an average of 10 individual measurements and are correct to ± 0.2 V.

2.2. *Ab initio* calculations

The GAUSSIAN 94 [11] suite of programs was used for all calculations, which were carried out on Silicon Graphics Power Challenge. The geometries of the local minima and the transition states were optimised at the RHF/6-31+G(d) and MP2 (Fc)/6-31+G(d,p) levels of theory. Harmonic frequency analyses were performed on each stationary point in order to characterise them as either a local minimum or transition state. A local minimum is characterised by possessing all real vibrational frequencies and its hessian matrix possessing all positive eigenvalues. A transition state is characterised by possessing one (and only one) imaginary frequency and its hessian matrix possessing one (and only one) negative eigenvalue. Intrinsic reaction coordinate (IRC) calculations were per-

formed (beginning from both transition structures) to verify that each transition structure connected particular local minima. Final energies are quoted at the MP2 Fc/6-31+G(d) level of theory, and include a scaled (0.8929) zero point vibrational energy correction [that is based on the RHF/6-31+G(d) optimised geometry].

2.2.1. Unlabelled compounds

Tetrahydrofurfuryl alcohol, 3,4-dihydro-2H-pyran, cyclobutanol, and cyclopropylmethanol were commercial samples. Tetrahydro-2H-pyran-3-ol was prepared by hydroboration of 3,4-dihydro-2H-pyran using 9-BBN [12]. 2-(3-methoxypropyl)oxiran was formed from 5-methoxypent-1-ene and *meta*-chloroperbenzoic acid [13]. Methoxy derivatives used in this study were made by standard methods (compare below).

2.2.2. Labelled compounds

The 2H and ^{18}O labelled tetrahydrofurfuryl alcohol were available from a previous study [14]. Other labelled compounds were synthesised as outlined below. The purity of all products was established by 1H NMR and positive ion mass spectrometry. The extent of incorporation (of D and/or ^{18}O) was established by either positive or negative ion mass spectrometry. Alcohols were converted into their methyl ethers by a standard route cf. [13].

2.2.3. 3,3- D_2 -2-(3-methoxypropyl)oxiran

4-Pentenoic acid (0.5 g) was added dropwise to a suspension of lithium aluminium deuteride (0.24 g) in diethyl ether (10 cm^3), and the mixture heated at reflux for 2 h. The mixture was cooled to 0°C, aqueous hydrogen chloride (saturated, 1 cm^3) was added, the organic layer separated, the aqueous layer extracted with diethyl ether (3 \times 5 cm^3), the combined organic extracts dried ($MgSO_4$), concentrated in vacuo, and the residue distilled to yield 1,1- D_2 -4-pentenol (0.4 g, 90%), b.p. 140–142°C. The labelled pentenol was converted to the methyl ether and then to 3,3- D_2 -2-(3-methoxypropyl)oxiran by the standard route [13]: yield (0.4 g, 68%).

2.2.4. 2-(3-¹⁸O-methoxypropyl)oxiran

A mixture of 4-pentenoic acid (1 g), oxalyl chloride (1.14 cm³), N,N-dimethylformamide (1 drop) in diethyl ether (30 cm³) was allowed to stir at 20°C for 3 h. Removal of the solvent in vacuo followed by distillation yielded 4-pentenoyl chloride (0.83 g, 70%), which was added to a mixture of anhydrous tetrahydrofuran (10 cm³) and H₂¹⁸O (0.15 g, 96% ¹⁸O), the mixture allowed to stir at 20°C for 24 h, the solvent removed in vacuo and the residue treated with lithium aluminium hydride [as for pentenoic acid (above)] to yield pent-4-en-1-ol-¹⁸O (0.70 g), that was converted to 2-(3-¹⁸O-methoxypropyl)oxiran (0.55 g, 47%) by the standard route [13].

2.3. Condensed phase reactions

Products of the reactions outlined below were analysed using a Finnigan MAT GCQ mass spectrometer. Conditions: Column phase RTX-SMS (length 30 cm, ID 0.25, GC fused silica capillary), He carrier gas. Initial column temperature, held at 50°C for 2 min, then the temperature increases at 15°C per minute. Retention times: **4** (5.39 min) and **5** (3.58 min).

A mixture of the acetate of **3** (0.5 g), in aqueous sodium hydroxide (10%, 5 cm³) was allowed to stir at 20°C (or 100°C—see Table 2) for 60 hours. The reaction mixture was sampled at various times. Each sample was acidified with aqueous hydrogen chloride (10%) until the pH was 6, extracted with dichloromethane (5 cm³), the organic extract dried (MgSO₄), and concentrated. The product composition was analysed by gc/ms (see Table 2).

Tetrahydro-2-furanmethanol (tetrahydrofurfuryl alcohol) and tetrahydropyran-3-ol were treated with aqueous sodium hydroxide as detailed in Table 2. No reaction was observed in either case.

3. Results and discussion

3.1. The results of ab initio calculations

The results of an ab initio computational study using GAUSSIAN 94 [11] for the reactions shown in

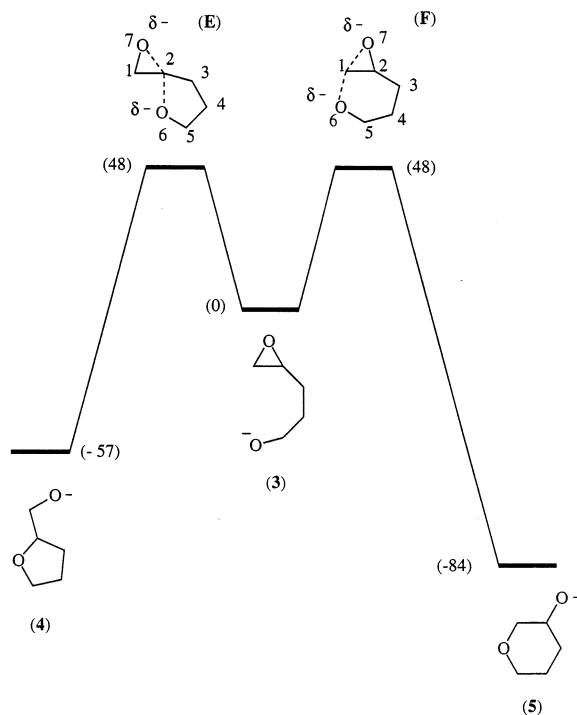


Fig. 1. Ab initio calculations at MP2-Fc/6-31+G(d) level (GAUSSIAN 94) for the reactions **3** → **4** and **3** → **5**. Energies, kJ mol⁻¹. Structures **3**, **4**, and **5** have a number of stable conformers. Those shown are the most stable (see Appendix for geometries and energies of the most stable conformers).

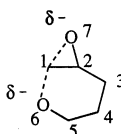
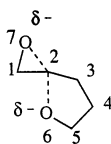
Scheme 2 are shown in Fig. 1. The geometries of the local minima and the transition states were optimised at the RHF/6-31+G(d) level of theory, and subsequently at the MP2-Fc/6-31+G(d) level of theory. Energies of **3**–**5**, **E**, and **F** together with the geometries of the two transition states are listed in Table 1. Full geometric data are listed in the appendix.

The details shown in Fig. 1 and Table 1 show the barriers to the two transition states **E** and **F** are both 48 kJ mol⁻¹ at the level of theory indicated. (It is of interest that a theoretical investigation of the gas phase reaction of HO⁻ with propylene oxide indicates that S_N2 addition can occur at either of the ring carbons, with reaction at the less substituted carbon being favoured marginally [15].) Factors that may contribute to these barriers are as follows. (1) The OCO angles in the transition states for the five- and six-centre rearrangements are 156.0 and 152.8°, with

Table 1

Energies of species shown in Fig. 1 and geometries of transition states **E** and **F**

Species	Energies [hartrees (kJ mol ⁻¹)]	Geometries
3	-308.167127 (nominally 0)	See Appendix
4	-345.1713646 (-57.1)	See Appendix
5	-345.1815112 (-83.7)	See Appendix
E	-345.1313611 (+48.0)	C ₁ C ₂ 1.4461 Å C ₂ C ₃ 1.5061 C ₃ C ₄ 1.5290 C ₄ C ₅ 1.5323 C ₅ O ₆ 1.3789 O ₆ C ₂ 2.1019 C ₂ O ₇ 1.7989 C ₁ C ₂ C ₃ 121.38° C ₂ C ₃ C ₄ 111.18 C ₃ C ₄ C ₅ 107.74 O ₆ C ₂ O ₇ 156.08 C ₂ O ₇ C ₁ 51.77 O ₇ C ₁ C ₂ 77.73 O ₆ C ₂ C ₁ O ₇ -176.13
F	-345.1314998 (+47.7)	C ₁ C ₂ 1.4374 Å C ₂ C ₃ 1.5128 C ₃ C ₄ 1.5348 C ₅ O ₆ 1.3786 O ₆ C ₁ 2.1044 C ₁ O ₇ 1.7644 O ₇ C ₂ 1.4261 C ₁ C ₂ C ₃ 115.69° C ₂ C ₃ C ₄ 109.68 C ₃ C ₄ C ₅ 112.91 C ₄ C ₅ O ₆ 114.70 O ₆ C ₁ O ₇ 152.82 C ₁ O ₇ C ₂ 76.07 O ₇ C ₂ C ₁ 119.62 O ₆ C ₁ C ₂ O ₇ 175.31



the dihedral angles being 176.1 and 175.3°, respectively. This should marginally favour the formation of the five-centre transition state, since previous studies [1–3] indicate that the closer the angles are to those of the “S_N2” state (180°), the more facile the reaction. (2) The release in ring strain in effecting the five- and six-centre transition states favours the formation of the six-centre state (strain energy of ethylene oxide, tetrahydrofuran, and tetrahydropyran are 112.5, 25.1, and 6.3 kJ mol⁻¹, respectively [7]). (3) The larger electrophilicity of the more substituted carbon of the

Table 2

Base catalysed solution reactions of 1-acetoxy-4,5-epoxypentane, **4**, and **5**. Base, 10% aqueous sodium hydroxide^a

Reactant	Temp (°C)	Time (h)	Product ratio (4:5) ^b
Acetate of 3	20	0.08	95:5
	20	1.0	95:5
	20	60.0	95:5
	100	0.08	91:9
	100	1.0	91:9
4	100	1.0	100:0
	100	60.0	100:0
5	100	1.0	0:100
	100	60.0	0:100

^aFor experimental conditions see Sec. 2, Experimental.

^bThe title compound **3** is not detected under these experimental conditions. Hydrolysis of the acetate gives the anion of **3**, which immediately cyclises (in quantitative yield) to yield the listed products.

ethylene oxide ring in the reactant (according to Mulliken charge analyses, C₁ = 0.057, C₂ = 0.478), favours formation of the five-centre transition state. If the computed barriers (i.e. the kinetics) solely control the relative rates of the two reactions, the formation of both **4** and **5** should be facile, and they should be formed in comparable yield.

3.2. The reactions of **3**, **4**, and **5** in the condensed phase

The base catalysed reactions of the acetate of **3** have been carried out previously under a number of conditions [16]. The neutrals derived from **4** and **5** are both formed, with the former formed in the higher yield. We have repeated these base catalysed reactions of the acetate of **3**, together with similar reactions of **4** and **5** in 10% aqueous sodium hydroxide: The results are summarised in Table 2. The five-membered ring system **4** is formed preferentially at room temperature (**4:5** = 18:1) and there is no change in the product ratio with increasing time. At 100°C, the ratio of **4:5** = 10:1, again, with no change with increasing time. There is no conversion of either **4** or **5** to **3**, even when the reaction mixture is heated under reflux for 60 h.

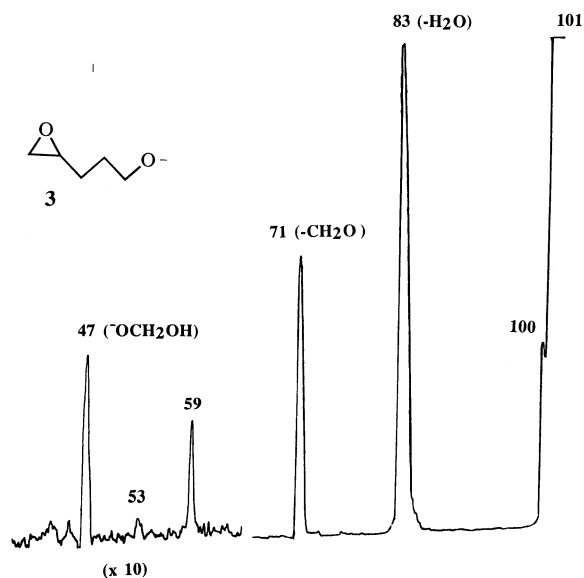


Fig. 2. Collision-induced mass spectrum (MS/MS) of **3**. Produced by the S_N2 reaction between the methyl ether and HO^- . VG ZAB 2HF instrument: For experimental conditions see Sec. 2, Experimental. Peak widths at half height [m/z (volts ± 0.2): 71 (25.2) and 83 (24.8).

3.3. Gas phase cyclisation of the 4,5-epoxypentoxide anion

All alkoxide anions were formed following S_N2 displacement from the precursor methyl ether: this is necessary since deprotonation of precursor alcohols can occur both at OH and elsewhere on the molecule. The collision-induced mass spectra of the three isomers **3**, **4**, and **5** are recorded in Figs. 2–4. Peak widths at half height for the major peaks in these spectra are recorded in the legend to each figure. Data pertaining to product ion studies are listed in Table 3, and the mass spectra of some 2H and ^{18}O labelled derivatives are recorded in Table 4.

The spectra of **3** and **4** shown in Figs. 1 and 2 are very similar, including identical peak widths at half height of the major fragment peaks at m/z 83 and 71. In contrast, the spectra of **3** and **4** are quite different from that of **5** (Fig. 3), and the heights at half height of m/z 83 and 71 in that spectrum are quite different from those in the spectra of **3** and **4**. This indicates that either the structures of m/z 83 and 71 from **5** are

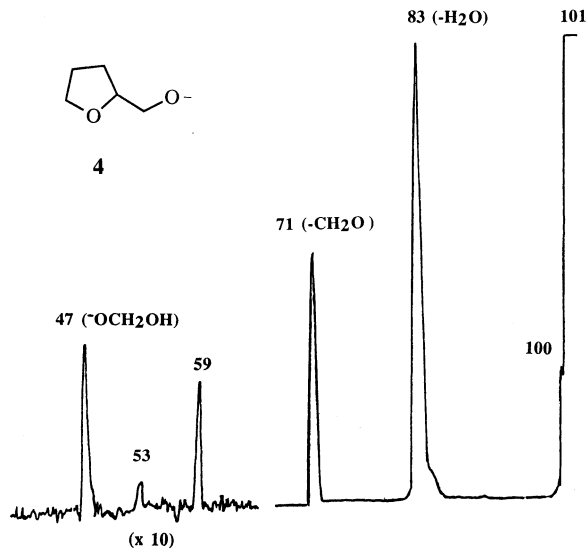


Fig. 3. Collision-induced mass spectrum (MS/MS) of **4**. Produced by the S_N2 reaction between the methyl ether and HO^- . VG ZAB 2HF instrument. Peak widths at half height [m/z (volts ± 0.2): 71 (25.3) and 83 (24.9).

different from the corresponding ions formed from **3** and **4**, and/or, that the mechanisms and energetics of the respective processes are different. This is the

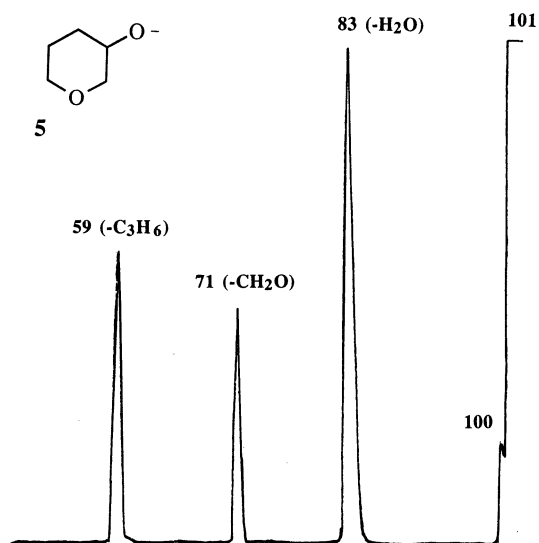
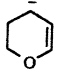

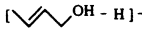
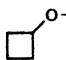


Fig. 4. Collision-induced mass spectrum (MS/MS) of **5**. Produced by the S_N2 reaction between the methyl ether and HO^- . VG ZAB 2HF instrument. Peak widths at half height [m/z (volts ± 0.2): 71 (29.5) and 83 (27.5).

Table 3
Product ion studies using charge reversal spectra^a

Parent ion (<i>m/z</i>)	Product ion (<i>m/z</i>)	Spectrum CR [<i>m/z</i> (abundance)]
3 (101)		100 (4), 81 (4), 71 (100), 69 (14), 57 (3), 55 (14), 53 (5), 45 (6), 43 (38), 42 (46), 41 (55), 39 (53), 31 (14), 29 (38), 27 (20).
4 (101)		100 (3), 81 (3), 71 (100), 69 (15), 57 (4), 55 (14), 53 (4), 45 (4), 43 (35), 42 (39), 41 (52), 39 (48), 31 (15), 29 (34), 27 (19).
5 (101)		100 (9), 71 (52), 69 (12), 55 (13), 53 (4), 45 (10), 43 (24), 42 (100), 41 (80), 39 (71), 31 (10), 29 (46), 27 (28).
3 (101)	–H ₂ O (83)	83 (31), 82 (100), 81 (52), 68 (12), 55 (40), 54 (28), 53 (43), 51 (23), 50 (21), 41 (7), 39 (55), 29 (30), 27 (28), 26 (10).
4 (101)	–H ₂ O	83 (33), 82 (100), 81 (60), 68 (14), 55 (50), 54 (33), 53 (55), 51 (28), 50 (28), 41 (10), 39 (66), 29 (30), 27 (32), 26 (14).
5 (101)	–H ₂ O (83)	83 (15), 82 (100), 81 (63), 68 (6), 55 (30), 54 (40), 53 (60), 51 (35), 50 (30), 49 (12), 39 (72), 29 (33), 27 (53), 26 (16).
	 (83) ^b	83 (26), 82 (100), 81 (66), 68 (5), 55 (48), 54 (32), 53 (60), 51 (30), 50 (30), 41 (12), 39 (58), 29 (32), 27 (37), 26 (15).
3 (101)	–CH ₂ O (71)	71 (4), 70 (46), 69 (75), 68 (15), 56 (21), 55 (52), 54 (32), 53 (35), 51 (14), 50 (16), 44 (6), 43 (24), 42 (65), 41 (78), 39 (100), 29 (42), 27 (36), 26 (16).
4 (101)	–CH ₂ O (71)	71 (2), 70 (52), 69 (72), 68 (15), 56 (20), 55 (45), 54 (28), 53 (30), 51 (12), 50 (13), 44 (6), 43 (19), 42 (65), 41 (78), 39 (100), 29 (42), 27 (36), 26 (16).
	 (71) ^c	71 (1), 70 (26), 69 (75), 68 (20), 56 (15), 55 (45), 54 (31), 53 (31), 51 (18), 50 (20), 44 (5), 43 (13), 42 (48), 41 (65), 39 (100), 29 (38), 27 (28), 26 (22).
	[ – H] ^d	71 (2), 70 (26), 69 (85), 68 (15), 56 (12), 55 (50), 54 (32), 53 (35), 51 (21), 50 (23), 44 (4), 43 (12), 42 (45), 41 (58), 39 (100), 29 (25), 27 (20), 26 (16).
5 (101)	–CH ₂ O (71)	71 (18), 70 (93), 69 (100), 68 (33), 55 (36), 42 (14), 41 (28), 39 (30), 29 (18), 27 (19).
	 (71) ^e	71 (12), 70 (88), 69 (100), 68 (36), 55 (37), 42 (14), 41 (25), 39 (28), 29 (14), 27 (20).
5 (101)	–C ₃ H ₆ (59)	59 (17), 58 (27), 56 (38), 45 (15), 44 (45), 42 (40), 41 (38), 31 (33), 30 (46), 29 (100), 28 (38).
	–OCH ₂ CHO ^f (59)	59 (10), 58 (24), 56 (38), 42 (42), 41 (40), 31 (31), 30 (44), 29 (100), 28 (39).
	CH ₃ CO ₂ ^g (59)	56 (4), 45 (28), 44 (100), 43 (36), 42 (38), 41 (18), 29 (12), 28 (15), 15 (10), 14 (5), 13 (2).

^aThese spectra are very dependent upon the collision gas pressure in the cell. Exact correspondence of abundances between spectra are not expected.

^bProduced by deprotonation of 3,4-dihydro-2H-pyran with HO[–] in the source.

^cProduced by deprotonation of cyclopropylmethanol by HO[–] in the source.

^dProduced by deprotonation of but-2-ene-1-ol by HO[–] in the ion source.

^eProduced by deprotonation of cyclobutanol by HO[–] in the source.

^fProduced by deprotonation of HOCH₂CHO with HO[–] in the ion source.

^gProduced by deprotonation of CH₃CO₂H with HO[–] in the ion source.

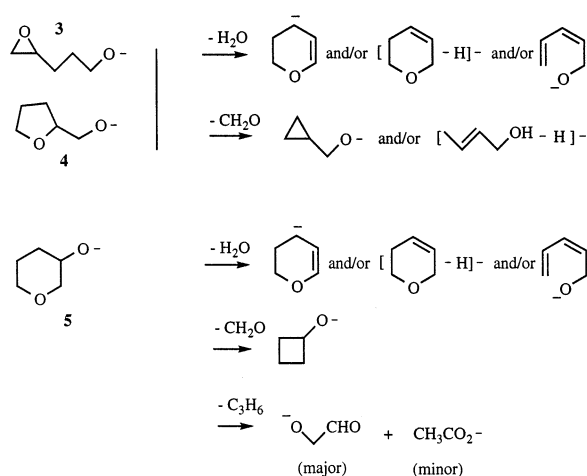
Table 4
CA MS/MS of labelled analogues^a [*m/z* (loss)abundance]

	102 (H ⁻)10, 101 (D ⁻)7, 85 (H ₂ O)100, 73 (CH ₂ O)34, 71 (CD ₂ O)68, 59 (C ₃ H ₄ D ₂)4, 49 (C ₄ H ₆)8, 47 (C ₄ H ₄ D ₂)4.
	102 (H ⁻)4, 101 (D ⁻)2, 85 (H ₂ O)100, 73 (CH ₂ O)43, 71 (CD ₂ O)12, 61 (C ₃ H ₆)49 49 (C ₃ H ₆)5, 47 (C ₄ H ₄ D ₂)3.
	102 (H ⁻)15, 85 (H ₂ O)70, 83 (H ₂ ¹⁸ O)97, 73 (CH ₂ O)61, 71 (CH ₂ ¹⁸ O)100, 61 (C ₃ H ₆)4, 49 (C ₄ H ₆)15.
	102 (H ⁻)15, 85 (H ₂ O)52, 83 (H ₂ ¹⁸ O)35, 73 (CH ₂ O)100, 71 (CH ₂ ¹⁸ O)37, 61 (C ₃ H ₆)6, 49 (C ₄ H ₆)12.

^aAnions produced by the S_N2 reaction between the methyl ether and HO⁻.

simplest scenario that we have seen in S_Ni studies to date cf. [1–3], viz. **3** is converting to **4** but that cyclisation to **5** is not occurring under the reaction conditions. We now need to confirm that (1) the fragment ions formed from **3** and **4** have the same structures, (2) there are differences between these structures and those of the fragment anions from **5**, and (3) fragmentations observed in the spectra of **3** occur following conversion to **4**.

The data concerning product ion studies are collected in Table 3. The collision activation spectra of source formed product anions are either not diagnostic in any of the cases under study, or the spectra are too weak for meaningful comparisons to be made. Thus we have compared the charge reversal spectra [10] of product anions with those of anions formed by independent syntheses. The results of these investigations are summarised in Scheme 3. Charge reversal spectra are positive ion spectra produced following charge stripping of the parent anion to yield a (decomposing) parent cation. Rearrangement reactions (particularly those involving movement of H) are more prevalent in positive ion spectra than negative ion spectra, thus care must be taken in using charge reversal spectra alone to determine the structure of the precursor negative ion. Sometimes charge reversal spectra provide an unequivocal answer; in other cases the situa-

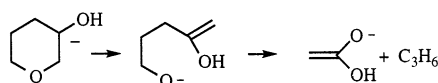


Scheme 3.

tion is more complex. Examples of both scenarios follow.

Loss of water from **3** and **4** give peaks (at *m/z* 83) with identical widths at half height and identical charge reversal spectra, thus the structure(s) and mechanism(s) of formation of these product anions are the same in both cases. The charge reversal spectra of *m/z* 83 from **3** and **4** are identical with that of deprotonated 3,4-dihydro-2H-pyran (see Table 3). However, the deprotonated forms of dihydropyran and the ring opened form shown in Scheme 3 will be in equilibrium under the reaction conditions, and charge reversal spectra will not differentiate between them. Loss of water from **5** gives a peak at *m/z* 83 that has a different width at half height when compared with those of the corresponding peaks from **3** and **4**, but the *m/z* 83 ions in all three spectra show identical charge reversal spectra.

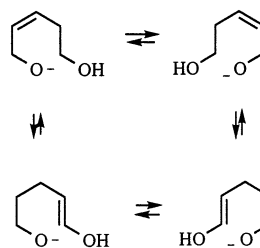
Data for the various losses of formaldehyde from **3**, **4**, and **5** (to form *m/z* 71) are more informative. Losses of CH₂O from **3** and **4** give peaks at *m/z* 71: their widths at half height and charge reversal spectra are identical. The charge reversal spectra of the *m/z* 71 ions from **3** and **4** and those of authentic deprotonated cyclopropylmethanol and but-2-en-1-ol are identical (see Table 3), thus *m/z* 71 from **3** and **4** correspond to either the cyclopropylmethoxide anion or the ring opened form of this species (see Scheme 3). There is a minor product formed by loss of CH₂O



Scheme 4.

from both **3** and **4** that gives rise to m/z 44 and 43 in the respective charge reversal spectra (see Table 3): this product has not been identified. In contrast, loss of formaldehyde from **5** gives a product anion (m/z 71) which has an identical charge reversal spectrum to that of deprotonated cyclobutanol (see Table 3). Finally, there is a pronounced peak at m/z 59 in the spectrum (Fig. 4) of **5** produced by loss of C_3H_6 . Comparison of the charge reversal spectrum of this ion with those of the formylmethoxy anion and the acetate anion (produced by deprotonation of glyoxal and acetic acid, respectively) show that both product anions are formed, with the formylmethoxy anion being the major product. The formation of the formylmethoxide anion is straightforward, but the acetate anion is an unexpected product. We propose the mechanism shown in Scheme 4 for the formation of the enol anion of the acetate anion (which will undergo internal proton transfer to form the thermodynamically more stable acetate anion).

The gas-phase data considered to date show that **3** and **4** have identical fragmentations, but they do not determine whether **3** cyclises to **4** before fragmentation occurs. In order to investigate this aspect of the problem we must consider the spectra of 2H and ^{18}O labelled derivatives of both the 4,5-epoxypentoxide and tetrahydro-2-furanmethoxide anions. These spectra are listed in Table 4. The spectra of the labelled derivatives demonstrate that (1) there is significant equilibration of the two oxygens before fragmentation of **3**, and (2) the extent of O equilibration preceding or accompanying fragmentation is consistent in the spectra of labelled **3** and **4**. (The 2H and ^{18}O labels in the labelled 4,5-epoxypentoxides following cyclisation, reside in the ring of the tetrahydro-2-furanmethoxide anion. In contrast, the 2H and ^{18}O derivatives of the tetrahydro-2-furanmethoxide anion from the labelled tetrahydrofurfuryl alcohol have the labels in the side chain. Thus the ratios $H_2O:H_2^{18}O$, $CH_2O:CH_2^{18}O$, and $CH_2O:CD_2O$, will be reversed in the two spectra.)



Scheme 5.

Such oxygen equilibration demands rearrangement of **3** prior to fragmentation.

We conclude from the presented data that **3** cyclises to **4** and that all fragmentations shown in Figs. 2 and 3 are those of the tetrahydro-2-furanmethoxide anion **4**. The fragmentations of **4** have been considered previously [14]. The spectrum shown in Fig. 3 looks deceptively simple; in fact, the processes preceding and accompanying fragmentation are complex. The losses of water and formaldehyde must come from equilibrating intermediates formed following ring opening of **4** cf. [14]. Four of these (which can interconvert by a series of proton transfers) are shown in Scheme 5. These can account both for the oxygen equilibration, and the product ion structures summarised in Scheme 2.

4. Summary and calculation of Arrhenius factors

The experimental results and ab initio calculations appear to be at variance. Ab initio results indicate that the barriers to the formation of **4** and **5** from **3** are small and comparable. If the barrier heights alone are controlling the rates of these kinetically controlled reactions, then both **4** and **5** should be formed in comparable proportions. Reaction in the condensed phase does form both **4** and **5**, but **4** is formed in significantly higher yield. In contrast, **3** forms **4** exclusively in the gas phase: there is no evidence for the formation of **5** from **3** in the gas phase.

This is the first occasion in our studies of S_Ni reactions where ab initio calculations seem to predict a different outcome to that obtained experimentally. However, a reaction rate is controlled by both the

barrier to the transition state and by the frequency or probability factor (or Arrhenius A factor). We have considered the qualitative effect of the A factors for competitive S_{Ni} reactions forming four- and five-membered rings in a previous study, but were unable to demonstrate that these were major factors in determining relative rates [3]. In the current system, because the barriers to the transition states are not controlling the relative rates of the reactions, the frequency factors must be. The two S_{Ni} reactions are concerted processes, and frequency factors for these competitive processes may be influenced by (1) the initial nucleophilic attack to form the transition state (i.e. the ability of the nucleophile to access the appropriate channel, and the depth of that channel), and/or (2) the nature of the transition state (i.e. whichever is “looser” (more disordered) will give the higher rate). To determine the relative abilities of the nucleophile to access the two channels requires an intimate knowledge of the potential surface maps for those processes (which we do not have), but the entropic natures of the two transition states may be determined by calculating the relative A factors.

To assess the relative Arrhenius A factors for the two competing cyclisation channels, we have used Transition State Theory [17], viz.

$$k(T) = (K_B T/h)(Q^\ddagger/Q_R) \exp(E_o/k_B T)$$

where k_B is Boltzman’s constant, h is Planck’s constant, E_o is the energy difference between reactant and transition state at 0°K, and Q^\ddagger and Q_R are the molecular partition functions of transition state and reactants, respectively. The partition function can be factorised into partition functions for translation, rotation, vibration, and electronic state [17], viz.

$$Q = Q_{\text{Trans}} \times Q_{\text{Rot}} \times Q_{\text{Vib}} \times Q_{\text{Elec}}$$

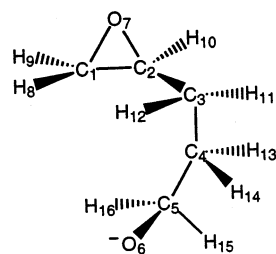
Since we are dealing with anions, it seems reasonable to assume that $Q_{\text{Elec}} = 1$. We are dealing with unimolecular rearrangements, so Q_{Trans} of the reactant and transition state are identical, and we assume (to a first approximation) that the same is true for Q_{Rot} . Thus, approximation of the A factor for each process simplifies to evaluating Q_{Vib} for the reactant and for the competing transition states. However, it must be noted that the anions in a mass spectrometer, especially following collisional activation, will not follow a Boltzman (thermalised) distribution of internal energies. Thus the following calculations must only be considered in a qualitative sense.

We have calculated, at the HF/6-31+G(d) level of theory, the harmonic vibrational frequencies of each structure using GAUSSIAN 94 cf. [18]. These values (scaled by a factor of 0.9131 [14]) are listed in the Appendix. A difficulty which often occurs with such an evaluation arises due to the problem of hindered rotors [19]. The calculated vibrational partition functions may underestimate the actual hindered rotor partition functions. Since we are concerned with the ratio of the A factors of two competing cyclisation channels that have the same reactant, we have not addressed the hindered rotor problem. The value of Q_{Vib}^\ddagger for the transition state leading to the five-membered ring product (**4**) is 20.5, whereas that for the six-membered product (**5**) is 10.2, so the transition state leading to the formation of (**4**) is “looser” than that giving (**5**). The rate of formation of (**4**) is thus predicted to be faster than that of (**5**) within the approximations we have employed.

Acknowledgements

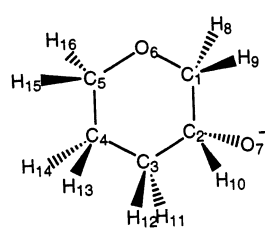
We thank the Australian Research Council for the financial support of this project.

**Appendix: Geometries of 3, 4, 5, E, and F [MP2-Fc/6-31+G(d), GAUSSIAN 94],
vibrational partition functions of 3, E, and FK**



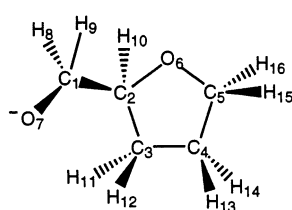
C ¹ C ²	1.4604Å
O ⁷ C ²	1.464
O ⁷ C ¹	1.4645
C ³ C ²	1.5017
H ⁸ C ¹	1.0892
H ¹⁰ C ²	1.0937
H ⁹ C ¹	1.0898
C ⁴ C ³	1.5312
H ¹¹ C ³	1.1013
H ¹² C ³	1.0949
C ⁵ C ⁴	1.5564
H ¹³ C ⁴	1.1064
H ¹⁴ C ⁴	1.0997
O ⁶ C ⁵	1.3575
H ¹⁵ C ⁵	1.1268
H ¹⁶ C ⁵	1.1301
C ¹ C ² O ⁷	60.1028°
C ² C ¹ O ⁷	60.072
C ² O ⁷ C ¹	59.8252
C ¹ C ² C ³	120.3024
O ⁷ C ² C ³	116.9503
C ² C ¹ H ⁸	116.398
O ⁷ C ¹ H ⁸	116.3269
C ¹ C ² H ¹⁰	117.6638
O ⁷ C ² H ¹⁰	112.1995
C ³ C ² H ¹⁰	116.6997
C ² C ¹ H ⁹	119.7241
O ⁷ C ¹ H ⁹	113.6938
H ⁸ C ¹ H ⁹	117.6178
C ² C ³ C ⁴	112.0927
C ² C ³ H ¹¹	109.3027
C ⁴ C ³ H ¹¹	111.5445
C ² C ³ H ¹²	107.7769
C ⁴ C ³ H ¹²	107.2884
H ¹¹ C ³ H ¹²	108.6918
C ³ C ⁴ C ⁵	111.2228
C ³ C ⁴ H ¹³	110.9791
C ⁵ C ⁴ H ¹³	110.4121
C ³ C ⁴ H ¹⁴	108.1068
C ⁵ C ⁴ H ¹⁴	108.4185

H ¹³ C ⁴ H ¹⁴	107.5667
C ⁴ C ⁵ O ⁶	113.3298
C ⁴ C ⁵ H ¹⁵	105.0059
O ⁶ C ⁵ H ¹⁵	114.5215
C ⁴ C ⁵ H ¹⁶	105.4858
O ⁶ C ⁵ H ¹⁶	113.833
H ¹⁵ C ⁵ H ¹⁶	103.6374
O ⁷ C ¹ C ² C ³	105.635
O ⁷ C ² C ¹ H ¹⁰	-100.9929
H ⁸ C ¹ C ² O ⁷	-106.5921
H ⁸ C ¹ C ² C ³	-0.9571
H ⁸ C ¹ C ² H ¹⁰	152.415
H ⁹ C ¹ C ² O ⁷	101.8442
H ⁹ C ¹ C ² C ³	-152.5208
H ⁹ C ¹ C ² H ¹⁰	0.8513
C ¹ O ⁷ C ² C ³	-111.1368
C ¹ O ⁷ C ² H ¹⁰	110.1085
C ² O ⁷ C ¹ H ⁸	106.7101
C ² O ⁷ C ¹ H ⁹	-111.8424
C ⁴ C ³ C ² C ¹	86.0768
C ⁴ C ³ C ² O ⁷	155.5574
C ⁴ C ³ C ² H ¹⁰	-67.5422
H ¹¹ C ³ C ² C ¹	-149.7222
H ¹¹ C ³ C ² O ⁷	-80.2416
H ¹¹ C ³ C ² H ¹⁰	56.6588
H ¹² C ³ C ² C ¹	-31.7599
H ¹² C ³ C ² O ⁷	37.7207
H ¹² C ³ C ² H ¹⁰	174.6211
C ⁵ C ⁴ C ³ C ²	-62.1188
C ⁵ C ⁴ C ³ H ¹¹	174.938
C ⁵ C ⁴ C ³ H ¹²	56.0084
H ¹³ C ⁴ C ³ C ²	61.2215
H ¹³ C ⁴ C ³ H ¹¹	-61.7216
H ¹³ C ⁴ C ³ H ¹²	-180.6513
H ¹⁴ C ⁴ C ³ C ²	178.9618
H ¹⁴ C ⁴ C ³ H ¹¹	56.0186
H ¹⁴ C ⁴ C ³ H ¹²	-62.911
O ⁶ C ⁵ C ⁴ C ³	-48.6745
O ⁶ C ⁵ C ⁴ H ¹³	-172.3384
O ⁶ C ⁵ C ⁴ H ¹⁴	70.058
H ¹⁵ C ⁵ C ⁴ C ³	-174.3756
H ¹⁵ C ⁵ C ⁴ H ¹³	61.9605
H ¹⁵ C ⁵ C ⁴ H ¹⁴	-55.6431
H ¹⁶ C ⁵ C ⁴ C ³	76.5035
H ¹⁶ C ⁵ C ⁴ H ¹³	-47.1605
H ¹⁶ C ⁵ C ⁴ H ¹⁴	-164.764



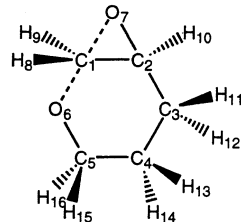
C ⁵ C ⁴	1.5232Å
C ³ C ⁴	1.5312
C ² C ³	1.5483
C ¹ C ²	1.5411
O ⁶ C ⁵	1.4232
O ⁶ C ¹	1.4577
O ⁷ C ²	1.3583
H ¹⁰ C ²	1.1282
H ¹² C ³	1.0984
H ¹¹ C ³	1.1015
H ¹³ C ⁴	1.0992
H ¹⁴ C ⁴	1.1029
H ¹⁶ C ⁵	1.1069
H ¹⁵ C ⁵	1.0976
H ⁸ C ¹	1.1041
H ⁹ C ¹	1.0934
C ⁵ C ⁴ C ³	110.0519
C ⁴ C ³ C ²	112.2756
C ³ C ² C ¹	106.7792
C ⁴ C ³ O ⁶	111.9446
C ² C ¹ O ⁶	115.0505
C ⁵ O ⁶ C ¹	110.4498
C ³ C ² O ⁷	113.965
C ¹ C ² O ⁷	110.8569
C ³ C ² H ¹⁰	105.4786
C ¹ C ² H ¹⁰	105.2
O ⁷ C ² H ¹⁰	113.9058
C ⁴ C ³ H ¹²	111.8285
C ² C ³ H ¹²	108.5085
C ⁴ C ³ H ¹¹	110.4077
C ² C ³ H ¹¹	106.5888
H ¹² C ³ H ¹¹	106.9548
C ⁵ C ⁴ H ¹³	108.1977
C ³ C ⁴ H ¹³	110.0775
C ⁵ C ⁴ H ¹⁴	109.145
C ³ C ⁴ H ¹⁴	111.9954
H ¹³ C ⁴ H ¹⁴	107.2617
C ⁴ C ³ H ¹⁶	109.4979
O ⁶ C ⁵ H ¹⁶	109.4982
C ⁴ C ⁵ H ¹⁵	111.8302
O ⁶ C ⁵ H ¹⁵	105.7616

H ¹⁶ C ⁵ H ¹⁵	108.1779
C ² C ¹ H ⁸	108.0651
O ⁶ C ¹ H ⁸	109.0874
C ² C ¹ H ⁹	109.9436
O ⁶ C ¹ H ⁹	105.6278
H ⁸ C ¹ H ⁹	108.9328
O ⁶ C ⁵ C ⁴ C ³	57.4147
O ⁶ C ⁵ C ⁴ H ¹³	62.8949
O ⁶ C ⁵ C ⁴ H ¹⁴	-180.6964
H ¹⁶ C ⁵ C ⁴ C ³	64.2131
H ¹⁶ C ⁵ C ⁴ H ¹³	-175.4773
H ¹⁶ C ⁵ C ⁴ H ¹⁴	-59.0685
H ¹⁵ C ⁵ C ⁴ C ³	-175.8961
H ¹⁵ C ⁵ C ⁴ H ¹³	-55.5865
H ¹⁵ C ⁵ C ⁴ H ¹⁴	60.8223
C ² C ³ C ⁴ C ⁵	53.6727
C ² C ³ C ⁴ H ¹³	-65.4949
C ² C ³ C ⁴ H ¹⁴	175.2712
H ¹² C ³ C ⁴ C ⁵	175.9231
H ¹² C ³ C ⁴ H ¹³	56.7555
H ¹² C ³ C ⁴ H ¹⁴	-62.4784
H ¹¹ C ³ C ⁴ C ⁵	-65.1167
H ¹¹ C ³ C ⁴ H ¹³	175.7157
H ¹¹ C ³ C ⁴ H ¹⁴	56.4818
C ¹ C ² C ³ C ⁴	-50.6
C ¹ C ² C ³ H ¹²	-174.7155
C ¹ C ² C ³ H ¹¹	70.4117
O ⁷ C ² C ³ C ⁴	-173.35
O ⁷ C ² C ³ H ¹²	62.5345
O ⁷ C ² C ³ H ¹¹	-52.3382
H ¹⁰ C ² C ³ C ⁴	60.9709
H ¹⁰ C ² C ³ H ¹²	-63.1446
H ¹⁰ C ² C ³ H ¹¹	-178.0173
O ⁶ C ¹ C ² C ³	53.9229
O ⁶ C ¹ C ² O ⁷	178.5944
O ⁶ C ¹ C ² H ¹⁰	-57.8404
H ⁸ C ¹ C ² C ³	-68.2266
H ⁸ C ¹ C ² O ⁷	56.4449
H ⁸ C ¹ C ² H ¹⁰	180.0101
H ⁹ C ¹ C ² C ³	172.9958
H ⁹ C ¹ C ² O ⁷	-62.3327
H ⁹ C ¹ C ² H ¹⁰	61.2325
C ¹ O ⁶ C ⁵ C ⁴	59.3675
C ¹ O ⁶ C ⁵ H ¹⁶	-62.2602
C ¹ O ⁶ C ⁵ H ¹⁵	-178.6078
C ⁵ O ⁶ C ¹ C ²	-59.6092
C ⁵ O ⁶ C ¹ H ⁸	61.9878
C ⁵ O ⁶ C ¹ H ⁹	178.9441



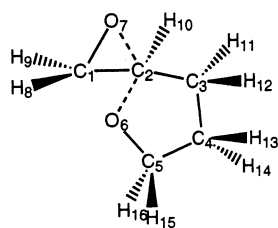
C ² O ⁶	1.4774 Å
C ³ C ²	1.535
C ⁴ C ³	1.5315
C ⁵ O ⁶	1.4246
C ⁵ C ⁴	1.5233
H ¹⁴ C ⁴	1.0979
H ¹² C ³	1.0968
H ¹¹ C ³	1.0935
C ¹ C ²	1.5371
H ¹⁰ C ²	1.0978
H ¹⁶ C ⁵	1.0974
H ¹⁵ C ⁵	1.1033
H ¹³ C ⁴	1.0981
H ⁸ C ¹	1.1231
O ⁷ C ¹	1.3613
H ⁹ C ¹	1.1317
O ⁶ C ² C ³	105.5317
C ² C ³ C ⁴	104.2065
C ² O ⁶ C ⁵	108.1137
C ³ C ⁴ C ⁵	100.8711
O ⁶ C ⁵ C ⁴	104.5849
C ³ C ⁴ H ¹⁴	111.1285
C ⁵ C ⁴ H ¹⁴	109.3427
C ² C ³ H ¹²	108.5352
C ⁴ C ³ H ¹²	111.3969
C ² C ³ H ¹¹	112.0083
C ⁴ C ³ H ¹¹	113.6855
H ¹² C ³ H ¹¹	106.9725
O ⁶ C ² C ¹	113.0199
C ³ C ² C ¹	111.6875
O ⁶ C ² H ¹⁰	105.715
C ³ C ² H ¹⁰	111.8728
C ¹ C ² H ¹⁰	108.8738
O ⁶ C ⁵ H ¹⁶	107.6792
C ⁴ C ⁵ H ¹⁶	114.5723
O ⁶ C ⁵ H ¹⁵	110.8683
C ⁴ C ⁵ H ¹⁵	110.4495
H ¹⁶ C ⁵ H ¹⁵	108.6073
C ³ C ⁴ H ¹³	113.707
C ⁵ C ⁴ H ¹³	113.2265
H ¹⁴ C ⁴ H ¹³	108.4015

C ² C ¹ H ⁸	106.182
C ² C ¹ O ⁷	110.9607
H ⁸ C ¹ O ⁷	115.0545
C ² C ¹ H ⁹	104.4273
H ⁸ C ¹ H ⁹	104.4276
O ⁷ C ¹ H ⁹	114.8515
C ³ C ² O ⁶ C ⁵	-12.5153
C ¹ C ² O ⁶ C ⁵	109.8163
H ¹⁰ C ² O ⁶ C ⁵	-131.1929
C ⁴ C ³ C ² O ⁶	-13.6589
C ⁴ C ³ C ² C ¹	-136.8422
C ⁴ C ³ C ² H ¹⁰	100.8285
H ¹² C ³ C ² O ⁶	105.1444
H ¹² C ³ C ² C ¹	-18.0389
H ¹² C ³ C ² H ¹⁰	-140.3682
H ¹¹ C ³ C ² O ⁶	-136.9769
H ¹¹ C ³ C ² C ¹	99.8398
H ¹¹ C ³ C ² H ¹⁰	-22.4895
C ⁵ C ⁴ C ³ C ²	32.5827
C ⁵ C ⁴ C ³ H ¹²	-84.25
C ⁵ C ⁴ C ³ H ¹¹	154.8029
H ¹⁴ C ⁴ C ³ C ²	-83.2529
H ¹⁴ C ⁴ C ³ H ¹²	159.9144
H ¹⁴ C ⁴ C ³ H ¹¹	38.9673
H ¹³ C ⁴ C ³ C ²	154.1108
H ¹³ C ⁴ C ³ H ¹²	37.278
H ¹³ C ⁴ C ³ H ¹¹	-83.669
C ⁴ C ⁵ O ⁶ C ²	34.0259
H ¹⁶ C ⁵ O ⁶ C ²	156.2968
H ¹⁵ C ⁵ O ⁶ C ²	-85.0229
O ⁶ C ⁵ C ⁴ C ³	-41.1607
O ⁶ C ⁵ C ⁴ H ¹⁴	75.9955
O ⁶ C ⁵ C ⁴ H ¹³	-163.0265
H ¹⁶ C ⁵ C ⁴ C ³	-158.8078
H ¹⁶ C ⁵ C ⁴ H ¹⁴	-41.6516
H ¹⁶ C ⁵ C ⁴ H ¹³	79.3264
H ¹⁵ C ⁵ C ⁴ C ³	78.1707
H ¹⁵ C ⁵ C ⁴ H ¹⁴	-164.673
H ¹⁵ C ⁵ C ⁴ H ¹³	-43.6951
H ⁸ C ¹ C ² O ⁶	56.1877
H ⁸ C ¹ C ² C ³	175.0088
H ⁸ C ¹ C ² H ¹⁰	-60.9584
O ⁷ C ¹ C ² O ⁶	-178.1251
O ⁷ C ¹ C ² C ³	-59.304
O ⁷ C ¹ C ² H ¹⁰	64.7288
H ⁹ C ¹ C ² O ⁶	-53.8438
H ⁹ C ¹ C ² C ³	64.9773
H ⁹ C ¹ C ² H ¹⁰	-170.9899



C ⁵ O ⁶	1.3786 Å
C ⁴ 5	1.5486
C ³ C ⁴	1.5348
C ² C ³	1.5128
C ¹ C ²	1.4374
O ⁷ C ²	1.4261
O ⁷ C ¹	1.7644
O ⁶ C ¹	2.1044
H ¹⁰ C ²	1.1003
H ¹² C ³	1.1022
H ¹¹ C ³	1.0994
H ¹⁴ C ⁴	1.1003
H ¹³ C ⁴	1.1044
H ¹⁵ C ⁵	1.1251
H ¹⁶ C ⁵	1.1158
H ⁸ C ¹	1.0807
H ⁹ C ¹	1.0801
O ⁶ C ¹ O ⁷	152.817°
O ⁶ C ⁵ C ⁴	114.6975
C ⁵ C ⁴ C ³	112.9088
C ⁴ C ³ C ²	109.6769
C ³ C ² C ¹	115.6918
C ³ C ² O ⁷	119.6248
C ¹ C ² O ⁷	76.0731
C ² C ¹ O ⁷	51.674
C ² O ⁷ C ¹	52.2529
C ³ C ² H ¹⁰	111.8615
C ¹ C ² H ¹⁰	115.5788
O ⁷ C ² H ¹⁰	113.8039
C ⁴ C ³ H ¹²	111.8532
C ² C ³ H ¹²	110.5602
C ⁴ C ³ H ¹¹	109.9397
C ² C ³ H ¹¹	107.5837
H ¹² C ³ H ¹¹	107.1604
C ⁵ C ⁴ H ¹⁴	107.5766
C ³ C ⁴ H ¹⁴	109.8593
C ⁵ C ⁴ H ¹³	109.345
C ³ C ⁴ H ¹³	109.5654
H ¹¹ C ³ H ¹²	107.4225
O ⁶ C ⁵ H ¹⁵	112.6773
C ⁴ C ⁵ H ¹⁵	105.6943

O ⁶ C ⁵ H ¹⁶	111.6769
C ⁴ C ⁵ H ¹⁶	106.4737
H ¹⁵ C ⁵ H ¹⁶	104.8966
C ² C ¹ H ⁸	119.1986
O ⁷ C ¹ H ⁸	102.1161
C ² C ¹ H ⁹	120.6656
O ⁷ C ¹ H ⁹	106.273
H ⁸ C ¹ H ⁹	119.2523
O ⁷ C ² C ¹ O ⁶	175.31
C ³ C ⁴ C ⁵ O ⁶	-65.5283
C ³ C ⁴ C ⁵ H ¹⁵	59.2229
C ³ C ⁴ C ⁵ H ¹⁶	170.4148
H ¹⁴ C ⁴ C ⁵ O ⁶	55.8528
H ¹⁴ C ⁴ C ⁵ H ¹⁵	-179.396
H ¹⁴ C ⁴ C ⁵ H ¹⁶	-68.2005
H ¹³ C ⁴ C ⁵ O ⁶	172.2174
H ¹³ C ⁴ C ⁵ H ¹⁵	-63.0314
H ¹³ C ⁴ C ⁵ H ¹⁶	48.1641
C ² C ³ C ⁴ C ⁵	57.8851
C ² C ³ C ⁴ H ¹⁴	-62.1949
C ² C ³ C ⁴ H ¹³	-179.9843
H ¹² C ³ C ⁴ C ⁵	-179.0724
H ¹² C ³ C ⁴ H ¹⁴	60.8476
H ¹² C ³ C ⁴ H ¹³	-56.9418
H ¹¹ C ³ C ⁴ C ⁵	-60.2156
H ¹¹ C ³ C ⁴ H ¹⁴	179.7045
H ¹¹ C ³ C ⁴ H ¹³	61.915
C ¹ C ² C ³ C ⁴	-65.7684
C ¹ C ² C ³ H ¹²	170.4289
C ¹ C ² C ³ H ¹¹	53.7864
O ⁷ C ² C ³ C ⁴	-153.8384
O ⁷ C ² C ³ H ¹²	82.3589
O ⁷ C ² C ³ H ¹¹	-34.2836
H ¹⁰ C ² C ³ C ⁴	69.4067
H ¹⁰ C ² C ³ H ¹²	-54.396
H ¹⁰ C ² C ³ H ¹¹	-171.0385
O ⁷ C ¹ C ² C ³	-116.4787
O ⁷ C ¹ C ² H ¹⁰	110.0182
H ⁸ C ¹ C ² C ³	-34.2527
H ⁸ C ¹ C ² O ⁷	82.226
H ⁸ C ¹ C ² H ¹⁰	-167.7559
H ⁹ C ¹ C ² C ³	156.5856
H ⁹ C ¹ C ² O ⁷	-86.9358
H ⁹ C ¹ C ² H ¹⁰	23.0824
C ¹ O ⁷ C ² C ³	111.8894
C ¹ O ⁷ C ² H ¹⁰	-112.1355
C ² O ⁷ C ¹ H ⁸	-117.7957
C ² O ⁷ C ¹ H ⁹	116.5204



O^7C^2	1.7989 Å	$C^5C^4H^{13}$	108.4477
O^6C^2	2.1019	$C^3C^4H^{14}$	111.0922
O^7C^1	1.4207	$C^5C^4H^{14}$	113.5391
C^2C^1	1.4461	$H^{13}C^4H^{14}$	107.9203
C^2O^{7r}	1.7989	$C^4C^5H^{11}$	107.6176
C^3C^2	1.5061	$O^6C^5H^{11}$	113.2684
C^4C^3	1.529	$C^4C^5H^{12}$	109.2839
C^5C^4	1.5323	$O^6C^5H^{16}$	113.1448
O^6C^5	1.3789	$H^{15}C^6H^{12}$	105.6161
H^8C^1	1.1006	$O^7C^1C^2O^6$	-176.131
$H^{10}C^2$	1.0814	$C^2O^7C^1H^8$	113.1821
H^9C^1	1.0984	$C^2O^7C^1H^9$	-114.5317
$H^{15}C^3$	1.0971	$O^7C^2C^1H^8$	-112.6824
$H^{16}C^3$	1.0993	$O^7C^2C^1H^9$	113.1519
$H^{13}C^4$	1.0995	$C^3C^2C^1O^7$	81.1691
$H^{14}C^4$	1.1039	$C^3C^2C^1H^8$	-31.5133
$H^{11}C^5$	1.1209	$C^3C^2C^1H^9$	-165.679
$H^{12}C^5$	1.1154	$H^{10}C^2C^1O^7$	-81.9907
$O^7C^2O^6$	156.078°	$H^{10}C^2C^1H^8$	165.3269
$O^7C^1C^2$	77.7252	$H^{10}C^2C^1H^9$	31.1612
$C^1O^7C^2$	51.767	$C^3C^2O^7C^1$	-119.9086
$C^1C^2O^7$	50.5078	$H^{10}C^2O^7C^1$	115.9088
$C^1C^2C^3$	121.3847	$C^4C^3C^2C^1$	133.716
$O^7C^2C^3$	103.3009	$C^4C^3C^2O^7$	-174.6941
$C^2C^3C^4$	111.176	$C^4C^3C^2H^{10}$	-63.5418
$C^3C^4C^5$	106.1834	$H^{15}C^3C^2C^1$	-103.178
$C^4C^5O^6$	107.7423	$H^{15}C^3C^2O^7$	-51.5882
$O^7C^1H^8$	115.587	$H^{15}C^3C^2H^{10}$	59.5642
$C^2C^1H^8$	116.0242	$H^{16}C^3C^2C^1$	12.8588
$C^1C^2H^{10}$	116.9532	$H^{16}C^3C^2O^7$	64.4486
$O^7C^2H^{10}$	101.0939	$H^{16}C^3C^2H^{10}$	175.601
$C^3C^2H^{10}$	119.4903	$C^5C^4C^3C^2$	-45.6864
$O^7C^1H^9$	116.0329	$C^3C^2C^3H^{15}$	-167.7106
$C^2C^1H^9$	117.2485	$C^5C^4C^3H^{16}$	74.1
$H^8C^1H^9$	110.8383	$H^{13}C^4C^3C^2$	71.2531
$C^2C^3H^{15}$	109.3039	$H^{13}C^4C^3H^{15}$	-50.7711
$C^4C^3H^{15}$	111.1774	$H^{13}C^4C^3H^{16}$	-168.9605
$C^2C^3H^{16}$	108.1727	$H^{14}C^4C^3C^2$	-169.5801
$C^4C^3H^{16}$	109.9835	$H^{14}C^4C^3H^{15}$	68.3956
$H^{15}C^3H^{16}$	106.8882	$H^{14}C^4C^3H^{16}$	-49.7937
$C^3C^4H^{13}$	109.5934	$O^6C^5C^4C^3$	47.463
		$O^6C^5C^4H^{13}$	-70.241
		$O^6C^5C^4H^{14}$	169.8173
		$H^{11}C^5C^4C^3$	-75.0018
		$H^{11}C^5C^4H^{13}$	167.2942
		$H^{11}C^5C^4H^{14}$	47.3525
		$H^{12}C^5C^4C^3$	170.7725
		$H^{12}C^5C^4H^{13}$	53.0685
		$H^{12}C^5C^4H^{14}$	-66.8732

HF/6-31+G(d) Harmonic Frequencies				
	(1/w)	3→6 ts HF	3→5 HF	Reactant
298	0.9131	5v6		
		157.437	96.8503	2.877577654
		248.9617	218.6748	1.616428524
		328.6974	259.2397	1.468223202
		349.07031	293.1267	1.378646413
		368.26711	318.8512	1.324862665
		456.6176	437.773	1.169807196
		474.7492	466.3916	1.14672652
		576.9262	595.4249	1.078101978
		851.9635	904.8141	1.01886973
		907.2457	939.6597	1.016139314
		957.8098	968.7445	1.014169573
		1020.9847	993.959	1.012660017
		1027.1873	1050.7703	1.009827594
		1088.694	1095.7603	1.008045302
		1098.9146	1139.4047	1.006627807
		1142.056	1184.6318	1.005423233
		1215.2838	1241.5412	1.004214805
		1251.3729	1241.7007	1.00421183
		1261.6875	1280.2103	1.003551853
		1306.8693	1316.6557	1.003023068
		1334.2357	1339.504	1.002732605
		1351.2783	1345.4006	1.002662299
		1388.4798	1377.3043	1.002312184
		1420.5572	1416.608	1.001943623
		1474.7671	1462.241	1.001588874
		1485.8614	1483.9876	1.001443413
		1528.1011	1516.9297	1.001248059
		1552.6904	1580.119	1.000944325
		1611.453	1616.8304	1.000803105
		1631.6319	1633.5746	1.000745915
		1643.413	1655.9089	1.000675924
		1658.3677	1694.1428	1.000571018
		2869.8021	2898.9173	1.000002817
		2959.1501	2959.6052	1.000002156
		3117.2053	3138.95	1.000000978
		3138.4509	3142.7375	1.000000961
		3154.7416	3167.9556	1.00000086
		3163.7017	3175.4567	1.000000832
		3194.9892	3206.0572	1.000000727
		3432.0823	3246.3859	1.000000609
		3552.7109	3487.5424	1.00000021
			10.16522992	20.41734345
			HF/6-31+G(d) Rotational Constants [GHz]	
Reactant	4.88875881	1.7928184	1.4219866	

Harmonic vibrational frequencies [hf/6-31+G(d)] of the competing transition states

TS forming 5 membered ring ν [cm^{-1}]	TS forming 6 membered ring ν [cm^{-1}]
96.8503	157.4370
218.6748	248.9617
259.2397	328.6974
293.1267	349.0703
318.8512	368.2671
437.7730	456.6176
466.3916	474.7492
595.4249	576.9262
904.8141	851.9635
939.6597	907.2457
968.7445	957.8098
993.9590	1020.9847
1050.7703	1027.1873
1095.7603	1088.6940
1139.4047	1098.9146
1184.6318	1142.0560
1241.5412	1215.2838
1241.7007	1251.3729
1280.2103	1261.6875
1316.6557	1306.8693
1339.5040	1334.2357
1345.4006	1351.2783
1377.3043	1388.4798
1416.6080	1420.5572
1462.2410	1474.7671
1483.9876	1485.8614
1516.9297	1528.1011
1580.1190	1552.6904
1616.8304	1611.4530
1633.5746	1631.6319
1655.9089	1643.4130
1694.1428	1658.3677
2898.9173	2869.8021
2959.6052	2959.1501
3138.9500	3117.2053
3142.7375	3138.4509
3167.9556	3154.7416
3175.4567	3163.7017
3206.0572	3194.9892
3246.3859	3432.0823
3487.5424	3552.7109

References

- [1] S. Dua, M.S. Taylor, M.A. Buntine, J.H. Bowie, *J. Chem. Soc. Perkin Trans. 2*, (1997) 1991.
- [2] S. Dua, M. S. Taylor, M.A. Buntine, J.H. Bowie, *Int. J. Mass Spectrom. Ion Processes*, 165/166 (1997) 139.
- [3] J.M. Hevko, S. Dua, J.H. Bowie, M.S. Taylor, *J. Chem. Soc. Perkin Trans. 2*, (1998) 1629.
- [4] L. Tenud, S. Farooq, J. Seible, A. Eschenmoser, *Helv. Chim. Acta* 53 (1970) 2059; G. Stork, J.F. Cohen, *J. Am. Chem. Soc.* 596 (1974) 5270.
- [5] J.E. Baldwin, *J. Chem. Soc. Chem. Commun.* (1976) 734; J.E. Baldwin, *Further Perspectives in Organic Chemistry: A Ciba Foundation Symposium*, Elsevier, Amsterdam, 1978, p. 85.
- [6] C.D. Johnson, *Acc. Chem. Res.* 26 (1993) 476.
- [7] S.W. Benson, *Thermochemical Kinetics*, Wiley and Sons, New York, 1968, p. 181.
- [8] V.G. Instruments, Wythenshawe, Manchester, UK, Model ZAB 2HF.
- [9] M.B. Stringer, J.H. Bowie, J.L. Holmes, *J. Am. Chem. Soc.* 108 (1986) 3888.
- [10] J.H. Bowie, T. Blumenthal, *J. Am. Chem. Soc.* 97 (1975) 2959; J.E. Szulejko, J.H. Bowie, I. Howe, J.H. Beynon, *Int. J. Mass Spectrom. Ion Phys.* 13 (1980) 76.
- [11] M.J. Frisch, G.W. Trucks, H.B. Schlegel, P.M.W. Gill, B.G. Johnson, M.A. Robb, J.R. Cheeseman, T. Keith, G.A. Petersen, J.A. Montgomery, K. Raghavachari, M.A. Al-Latham, V.G. Zakrewski, J.V. Ortiz, J.B. Foresman, J. Cioslowski, B.B. Stefanov, A. Nanayakkara, M. Challacombe, C.Y. Peng, P.V. Ayala, W. Chen, M.W. Wong, J.L. Andres, E.S. Replogle, R. Gomperts, R.L. Martin, D.J. Fow, J.S. Binkley, D.J. Defrees, J. Baker, J.P. Stewart, M. Head-Gordon, C. Gonzales, J.A. Pople, *GAUSSIAN 94*, Revision C3, Gaussian Inc., Pittsburgh, PA, 1995.
- [12] H.C. Brown, J.V.N. Vara Prasad, S. Zee, *J. Org. Chem.* 50 (1985) 1582.
- [13] Y. Masaki, T. Muira, I. Mukai, A. Itoh, H. Oda, *Chem. Lett.* (1991) 1937.
- [14] S. Dua, R.A.J. O'Hair, J.H. Bowie, R.N. Hayes, *J. Chem. Soc. Perkin Trans. 2*, (1992) 1151.
- [15] S. Gronert, J.M. Lee, *J. Org. Chem.* 60 (1995) 4488.
- [16] M.L. Mihailovic, D. Marinkovic, *Croatica Chem. Acta* 59 (1986) 109.
- [17] R.G. Gilbert, S.C. Smith, *Theory of Unimolecular and Recombination Reactions*, Blackwell Scientific, Cambridge, 1990.
- [18] A.P. Scott, L. Radom, *J. Phys. Chem.* 100 (1996) 16502.
- [19] J.P.A. Heuts, R.G. Gilbert, L. Radom, *Macromolecules* 28 (1995) 8771; *J. Phys. Chem.* 100 (1996) 18997.